ISSN 2176-5480

22nd International Congress of Mechanical Engineering (COBEM 2013)
November 3-7, 2013, Ribeirão Preto, SP, Brazil

NUMERICAL APPROXIMATIONS FOR THE STRUCTURED THIXOTROPIC FLUIDS IN AN ABRUPT PLANAR EXPANSION

Cleiton Fonseca
Sérgio Frey
Department of Mechanical Engineering, Federal University of Rio Grande do Sul Rua Sarmento Leite 425, Porto Alegre, RS 90050-170, Brazil
cfonseca@mecanica.ufrgs.br
frey@mecanica.ufrgs.br

Mônica F. Naccache
Paulo R. de Souza Mendes
Department of Mechanical Engineering, Pontifícia Universidade Católica-RJ Rua Marquês de São Vicente 225, Rio de Janeiro, RJ 22453-900, Brazil
naccache@puc-rio.br
pmendes@puc-rio.br

Abstract. *A numerical investigation of a structured thixotropic fluid flowing in an abrupt planar expansion is performed, using the recently model proposed by de Souza Mendes (2009). This model present a Maxwell-type constitutive equation where the relaxation time and the viscosity are dependent of the material structure level. The structure level is determined through to a time dependent evolution equation. The model equations are approximated by the stabilized Galerkin Least-square Method. The numerical research presented consistent results for the Structured Thixotropic Fluid flows where the relevant parameters for the model are varied.*

Keywords: *Structured Thixotropic Fluids, thixotropy, elasticity, viscoplasticity, Galerkin Least-square Methods*

1. INTRODUCTION

Many industrial and scientific activities involving Structured Thixotropic Fluid which makes the study of their behavior of great importance. The main characteristics of Structured Thixotropic Fluids are: (i) structure-dependent viscosity; (ii) elastic effects to high levels of structuring the material; (iii) unyielded regions to high structure levels; (iv) time-dependent tixotropic effects. Examples of the Structure Thixotropic Fluids include emulsions, paints, nanocomposites, gels, drilling fluids, food products, and mineral slurries. The aim of the present article is to analyze the performance in a complex flow of the constitutive equation for Structured Thixotropic Fluids recently proposed by de Souza Mendes (2009). This equation is based on the upper-convected Maxwell constitutive equation, modified to include structuring level dependence in both the elastic modulus and the viscosity. It is introduced in the model a parameter that describes the material structure level governed by an evolution equation. The numerical modeling of the governing equations is based on a four-field Galerkin least-squares formulation in terms of the structure parameter, extra-stress, pressure, and velocity. The formulation mentioned above is used to perform a numerical investigation of the steady flow of a Structured Thixotropic Fluid flowing in an abrupt planar expansion. Inertia is neglected, and thixotropic and elastic effects are evaluated for a relevant range of the governing parameters. All the numerical results proved to be physically meaningful and in accordance with the related literature, indicating that the constitutive equation employed provides a good description of the mechanical behavior of elasto-viscoplastic thixotropic fluids.

2. NUMERICAL SCHEME

2.1 Mechanical Model

According to the model proposed in de Souza Mendes (2009), assuming a open domain $\Omega \in \Re^2$, bounded by a regular polygonal boundary Γ, where it is assumed one creeping flow, the model for structured thixotropic fluid can be described by the equations of conservation of mass and balance of momentum, coupled with a Maxwell-type equation and a evolution equation for the level of material structure. Thus, we can write the mechanical model as follows

$$\partial_{x_k} u_k = 0 \quad \text{in } \Omega \tag{1}$$

$$\partial_{x_i}\mathcal{P} - \partial_{x_j}\tau_{ij} - 2\eta_\infty \partial_{x_j} D(u)_{ij} = 0 \ \text{ for } \ i = 1, \cdots N \quad \text{in } \Omega \tag{2}$$

$$\tau_{ij} + \theta(\lambda)\check{\tau}_{ij} - 2\eta(\lambda) D(u)_{ij} = 0 \ \text{ for } \ i,j = 1, \cdots N \quad \text{in } \Omega \tag{3}$$

$$u_k \partial_{x_k}\lambda = \frac{1}{t_{eq}}\left[(1-\lambda) - (1-\lambda_{eq})\left(\frac{\lambda}{\lambda_{eq}}\right)\left(\frac{\tau}{\eta(\lambda)\dot{\gamma}}\right)\right] \quad \text{in } \Omega \tag{4}$$

ISSN 2176-5480

where $\check{\tau}_{ij}$ stands for the upper-convected derivative of the extra-stress tensor,

$$\check{\tau}_{ij} = u_k \partial_{x_k} \tau_{ij} - \partial_{x_k} u_i \tau_{kj} - \tau_{ik} \partial_{x_k} u_j \tag{5}$$

and u_i is the component of velocity vector, $\mathcal{P}$ is the moficated pressure, D_{ij} is the component of strain rate tensor,

The relaxation time θ, the elastic modulus G and the structural viscosity η are functions of a scalar parameter λ that maps the material structuring level,

$$\theta(\lambda) = \frac{\eta(\lambda)}{G(\lambda)} \quad ; \quad G(\lambda) = \frac{G_0}{\lambda^m} \quad ; \quad \eta(\lambda) = \left(\frac{\eta_0}{\eta_\infty}\right)^{\lambda} \eta_\infty \tag{6}$$

with G_0 representing the elastic modulus of a fully-structured material and λ determined solving the evolution equation above,

$$u_k \partial_{x_k} \lambda = \frac{1}{t_{eq}} \left[(1-\lambda) - (1-\lambda_{eq}) \left(\frac{\lambda}{\lambda_{eq}}\right) \left(\frac{\tau}{\eta(\lambda)\dot{\gamma}}\right) \right] \tag{7}$$

The equilibrium-state of the structure parameter can be obtained from the equilibrium-state of the structural viscosity,

$$\lambda_{eq}(\dot{\gamma}_{eq}) = \frac{\ln \eta_{eq}(\dot{\gamma}_{eq}) - \ln \eta_\infty}{\ln \eta_0 - \ln \eta_\infty} \tag{8}$$

where η_{eq} is given by the viscoplastic viscosity function proposed in de Souza Mendes and Dutra (2004),

$$\eta_{eq}(\lambda_{eq}) = \left[1 - \exp(-\frac{\eta_0 \dot{\gamma}_{eq}}{\tau_0})\right] \left[\frac{\tau_0 - \tau_{0_d}}{\dot{\gamma}_{eq}} \exp(-\frac{\dot{\gamma}_0}{\dot{\gamma}_{0_d}}) + \frac{\tau_{0_d}}{\dot{\gamma}_{eq}} + K\dot{\gamma}_{eq}^{n-1}\right] + \eta_\infty \tag{9}$$

η_0 and η_∞ are the viscosity of fully structured and unstructured fluids, and τ_0 and τ_{0_d} are the static and dynamic yield stress.

2.2 Finite Elements Method

The numerical solution for a Structured Thixotropic Fluids flows is obtained using a multi-field Galerkin Least-Squares formulation (GLS) in terms of the structure parameter, extra-stress, velocity and pressure (Fonseca, 2013). In an attempt to increase the stability of classical Galerkin formulation, GLS formulation have with main features simple combinations of finite element interpolation and a stable approach for both elastic and viscous-dominated regions. Employing the usual finite element subspaces to the incompressible muti-fields problem - $\lambda \in H^1(\Omega)$, $\boldsymbol{\tau} \in C^0(\Omega)^{N\times N} \cap H^2(\Omega)^{N\times N}$, $p \in C^0(\Omega) \cap H^2(\Omega)$, $\boldsymbol{u} \in H^1(\Omega)^N$ - such a formulation is expressed as: *Find the quadruple* $(\lambda^h,\ \boldsymbol{\tau}^h,\ p^h,\ \boldsymbol{u}^h) \in \Lambda^h \times \Sigma^h \times P^h \times V^h_g$ *such that* $\forall\ (\phi^h\ , \boldsymbol{S}^h,\ q^h,\ \boldsymbol{v}^h) \in \Lambda^h \times \Sigma^h \times P^h \times V^h$

$$\begin{aligned}
&\int_\Omega (\nabla\cdot\mathbf{u^h}) q^h d\Omega + \varepsilon \int_\Omega p^h q^h d\Omega - \int_\Omega p^h (\nabla\cdot\mathbf{v^h}) d\Omega + \int_\Omega \boldsymbol{\tau}^h \cdot \mathbf{D}(\mathbf{v^h}) d\Omega \\
&+ \int_\Omega \boldsymbol{\tau}^h \cdot \mathbf{S^h} d\Omega - \int_\Omega 2\eta_v \mathbf{D}(\mathbf{u^h}) \cdot \mathbf{S^h} d\Omega - \int_\Omega \theta(\lambda) \boldsymbol{\tau}^h (\nabla \mathbf{u^h})^T \cdot \mathbf{S^h} d\Omega \\
&+ \int_\Omega \theta(\lambda^h)(\nabla \boldsymbol{\tau}^h)\mathbf{u^h} \cdot \mathbf{S^h} d\Omega - \int_\Omega \theta(\lambda^h)(\nabla \mathbf{u^h})\boldsymbol{\tau}^h \cdot \mathbf{S^h} d\Omega \\
&+ \int_\Omega (\mathbf{u^h}\cdot\nabla\lambda^h)\phi^h d\Omega + t_{eq}^{-1} \int_\Omega \lambda^h \phi^h d\Omega - t_{eq}^{-1} \int_\Omega \left[\frac{1-\lambda_{eq}}{\lambda_{eq}} \left(\frac{\tau}{\eta_v(\lambda)\dot{\gamma}}\right)^c\right] \lambda^h \phi^h d\Omega \\
&+ \int_\Omega (\nabla\cdot\mathbf{u^h})\delta(\nabla\cdot\mathbf{v^h}) \mathbf{d\Omega} + \sum_{\mathbf{K}\in\mathbf{\Omega^h}} \int_{\mathbf{\Omega_k}} (\nabla \mathbf{p^h} - \nabla\cdot\boldsymbol{\tau}^\mathbf{h}) \cdot \alpha(\mathbf{x})(\nabla \mathbf{q^h} - \nabla\cdot\mathbf{S^h}) \mathbf{d\Omega} \\
&+ \int_\Omega \left[\mathbf{u}\cdot\nabla\lambda^h + t_{eq}^{-1}\lambda^h - \left[\frac{1-\lambda_{eq}}{\lambda_e q}\left(\frac{\tau}{\eta_v(\lambda^h) dot\gamma}\right)^c\right]\lambda^h\right] \\
&\qquad\qquad \cdot\psi \left[\mathbf{u^h}\cdot\nabla\phi^h + t_{eq}^{-}1\phi^h - \left[\frac{1-\lambda_{eq}}{\lambda_{eq}}\left(\frac{\tau}{\eta_v(\lambda^h)\dot{\gamma}}\right)^c\right]\phi^h\right] d\Omega \\
&+ 2\eta_p \int_\Omega ((2\eta_p)^{-1}\boldsymbol{\tau}^h + (2\eta_p)^{-1}\theta(\lambda)((\nabla\boldsymbol{\tau}^h)\mathbf{u}^h - \nabla\mathbf{u}^h\boldsymbol{\tau}^h - \boldsymbol{\tau}^h\nabla(\mathbf{u}^h)^T) + \mathbf{D}(\mathbf{u})^h) \\
&\qquad\qquad \cdot\beta((2\eta_p)^{-1}\mathbf{S}^h + (2\eta_p)^{-1}\theta(\lambda)((\nabla\mathbf{S}^h)\mathbf{u}^h - \nabla\mathbf{u}^h\mathbf{S}^h - \mathbf{S}^h\nabla(\mathbf{u}^h)^T) - \mathbf{D}(\mathbf{v})^h) d\Omega \\
&= \int_\Omega \mathbf{f}\cdot\mathbf{v^h} d\Omega + \int_\Omega t_{eq}^{-1}\phi^h d\Omega + \int_{\Gamma_h} \mathbf{t}_h \cdot \mathbf{v^h} d\Gamma + \sum_{K\in\Omega^h} \int_{\Omega_K} \mathbf{f}\cdot\alpha(\mathbf{x})(-\nabla\mathbf{q^h} + \nabla\cdot\mathbf{S^h}) \mathbf{d\Omega}
\end{aligned} \tag{10}$$

ISSN 2176-5480

where stability parameters α and δ are proposed in Franca and Frey (1992) for fluids with constant viscosity, ψ is the parameter introduced in Franca et al. (1999) equation in the context of advection-reaction-diffusion, and the parameter β is set according to the error estimate GLS established in Behr et al. (1993). The discretization of Eq. 10 are obtained from the expansions of finite element approximations for λ^h, $\boldsymbol{\tau}^h$, $\mathbf{u^h}$, p^h, ϕ^h, $\mathbf{S^h}$, $\mathbf{v^h}$ and q^h as a combination of their respective shape functions and degrees of freedom, thus generating residual system of a nonlinear equations. In the solution of the algebraic system obtained is employed iterative Quasi-Newton Method.

2.3 Yield Surface Criterion

Structured Thixotropic Fluids flows have a two distinct regions: yielded region where the flow behaves as a Newtonian Generalized Liquid; unyielded region where the flow has a very high viscosity and elasticity effect. The surface that separates these two regions is called yield surface. In the literature there are numerous criteria to determine the yield surface, for example we can quote criteria yielded stress, bi-viscosity, yielded strain rate, etc. For Structured Thixotropic Fluids, none of these criteria would be physically correct due to the temporal dependence between the applied stress and the strain rate. For the fluid in question a physically correct criterion is to determine a level of structuring the material that would separate the two distinct regions mentioned above. To calculate the structure parameter must resolve the Eq.8 and thus determine a strain rate which characterizes the yield surface. One suitable physically choice is $\dot{\gamma}(\tau_0,\ \eta_0)$ given by the following expression:

$$\dot{\gamma}_0 = \frac{\tau_0}{\eta_0} \tag{11}$$

were the $\dot{\gamma}_0$ is the strain rate for the totally structured fluid.

2.4 Dimensionless Parameters

The equations and dimensionless parameters are obtained using a rheological adimensionalization proposed by de Souza Mendes, 2007. The adimensionalization has the virtue of decoupling of kinematic and rheological effects of dimensionless parameters coming from the of motion and material equations. Thus, we introduce the nondimensional variable set below

$$t^* = t\dot{\gamma}_1;\ \mathbf{x}^* = \frac{\mathbf{x}}{\mathbf{L_c}};\ \ \mathbf{u}^* = \frac{\mathbf{u}}{\dot{\gamma}_\mathbf{1}\mathbf{L_c}};\ \ \dot{\gamma}^* = \frac{\dot{\gamma}}{\dot{\gamma}_\mathbf{1}};\ \ \mathbf{p}^* = \frac{\mathbf{p}}{\tau_\mathbf{0}};\ \boldsymbol{\tau}^* = \frac{\boldsymbol{\tau}}{\tau_\mathbf{0d}};\ \ \eta^*_\mathbf{v}(\dot{\gamma}^*) = \frac{\eta_\mathbf{v}(\dot{\gamma})}{\tau_\mathbf{0d}/\dot{\gamma}_\mathbf{1}} \tag{12}$$

From the dimensionless equations governing the mechanical model arise important dimensionless numbers shown below

$$J \equiv \frac{\dot{\gamma}_1 - \dot{\gamma}_0}{\dot{\gamma}_0} = \eta^*_0 - 1;\ \ \theta^*_0 \equiv \theta^*(1) = \frac{\eta_0\dot{\gamma}_1}{G_0} = \frac{\tau_{0d}}{G_0}(J+1);\ \ U^* = \frac{U}{\dot{\gamma}_1 L_c} \tag{13}$$

where J is a measure of the jump of shear rate occurs when the material flows while the stress is approximately over τ_0, θ^*_0 is the relaxation time for a fully structured fluid and is elastic parameter of the problem and U^* is the intensity of the flow and is the parameter that carries the information about the kinematics of the flow.

2.5 Problem Statement

The geometry and boundary conditions are illustrated in Fig. **??**. The abrupt expansion has 50 L_c units upstream and downstream of the expansion plan, where L_c is equal to half the height of the channel upstream of the expansion plan. The length of the channels upstream and downstream of the expansion plan is considered sufficient in order to achieve a fully developed flow. The aspect ratio given by H_{in}/H_{out} is 1:4.

The kinematic boundary conditions are:

(i) no slip and tightness along the channel wall and the surface of the cylinder ($u_i = 0 \quad for\ i = 1, ..., N$);

(ii) symmetry along the center line of the channel ($\tau_{ij} = \partial_{x_j} u_i = 0 \quad for\ i \neq j \quad and \quad u_2 = 0$);

(iii) uniform profiles for velocity and extra stress along the channel input ($\tau_{ij} = 0 \quad for\ \ i, j = 1, ..., N \quad and \quad u_1 = U, u_2 = 0$)

(iv) free traction along the channel outlet ($[-\partial_{x_i} p + \tau_{12}]n_i = 0$)

(v) uniform profile along the channel inlet for the structure parameter ($\lambda = 0$)

ISSN 2176-5480

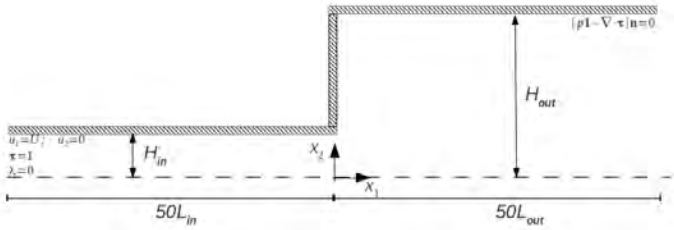

Figure 1. The geometry and the flow kinematics.

Remarks:

(i) Due to the parabolic nature of the evolution equation for the level of the material structure, only one initial condition is necessary. Thus, boundary conditions at the channel inlet are sufficient for your solution.

(ii) Other important topic that deserves attention concerns the imposition of kinematic boundary conditions along the entrance channel. Unlike purely viscoelastic or viscoplastic flow, for which appropriate exact solutions for fully developed stress and velocity profiles are available, an imposition of exact boundary conditions profiles is not possible for the Structured Thixotropic Fluids flow. Structured Thixotropic Fluid flows are neither purely viscoelastic nor purely viscoplastic, which makes the imposition of the input stress and velocity profiles an open question. Thus, we opted for flat profiles which caused some flow entry problems.

2.6 Mesh Independence

In order to evaluate the independence of the results in relation the mesh used for the simulations of Strutured Thixotropic Fluids flows in an abrupt planar expansion, it was made four bi-linear lagrangian meshes (Q1) with different refinements: (i) M1 mesh with 2500 elements (ii) M2 mesh with 5000 elements (iii) M3 mesh with 6500 elements (iv) M4 mesh with 7680 elements . To research the meshes made, it was decided to compare the transverse profiles of the structure parameter in the expansion plane. This choice becomes interesting by the fact that, as stated earlier, the parameter structure involves in its evolution equation (Eq. 4), the extra-stress tensor magnitude , structural viscosity, strain rate and thixotropic effects. The location of the profiles were chosen in areas which the main effects are experienced by the flow. The results are shown in Fig. **??** for the parameters fixed $\theta_0^* = 5$, $J = 500$, $n = 0.5$ and $t_{eq}^* = 1$.

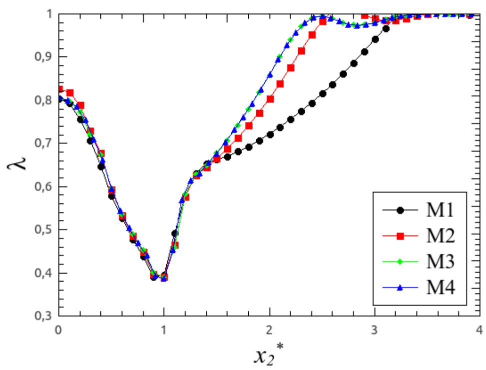

Figure 2. Structure Parameter profiles for $\theta_0^* = 5$, $J = 500$, $n = 0.5$, $t_{eq}^* = 1$ and $x_1^* = 0$

In the Tab. **??** show the calculation of relative error of the results obtained for the structure parameter profiles shown in Fig. **??**. The relative error is calculated between meshes, where is compared a lowest refinement mesh with a largest refinement mesh.

Table 1. Relative error for the structure parameter transverse profiles in $x_1^* = 0$

x_2^*	M1-M2	M2-M3	M3-M4
0	2.80%	2.64%	0.29%
0.5	2.46%	0.35%	0.22%
1	0.75%	0.48%	0.96%

Determining how mesh independence criterion a relative error of 1%, so we can assert that the M3 mesh refinement is

ISSN 2176-5480

sufficient. In Fig **??** is showed the mesh detail.

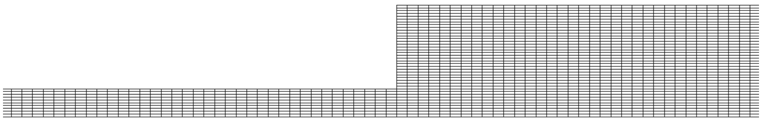

Figure 3. Bi-linear Finite Element mesh M3

3. RESULTS

In this section, numerical simulations of Structured Thixotropic Fluids flows are here obtained by stabilized finite element approximations of the governing equations defined by Eqs. 1, 2, 3 and 4. The numerical scheme introduced in the previous section is used to approximate creeping flows $(Re << 1)$ in steady state for Structured Thixotropic Fluids through a geometry of interest in engineering problems. Flow characteristics are presented and discussed for relevant ranges of the rheological and kinematic parameters governing the mechanical model.

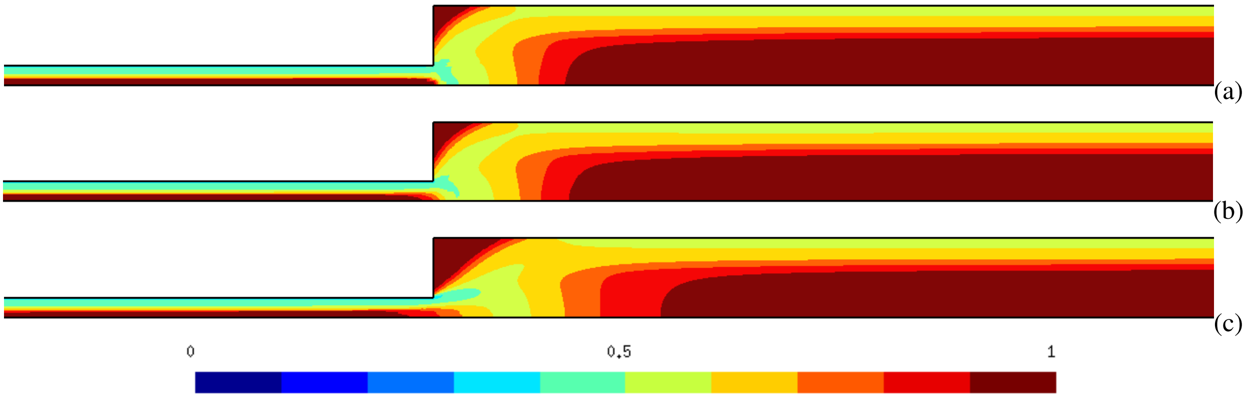

Figure 4. Structure Parameter field for $\theta_0^* = 5$, $J = 500$, $n = 0.5$ and: (a)$t_{eq}^* = 0.01$; (c) $t_{eq}^* = 1$ and (e) $t_{eq}^* = 10$

The Fig. **??** shows the influence to thixotropic effects of different flows. The kinematics, elasticity, shear thinning and viscosity levels are kept fixed. An increase in thixotropic effects causes the material structure present a major restructuring time to achieve equilibrium with the applied stress. The materials with higher thixotropy has a restructuring later after the breakage due the stress caused in the expansion, where the space acceleration of the structure parameter (advective term of Eq. 4) is higher. It is also observed that low levels of the material structure in the corner of expansion are advected into the channel.

The yielded/unyielded regions fields for an influence of the thixotropic effects investigation on Structured Thixotropic fluids flows in an abrupt planar expansion is shown in Fig.**??**. Determining the level of structuring of the fluid that delimits a yielded/unyielded regions in accordance with the procedures set forth in section 2.3, it was found the yield surface the locus where $\lambda \simeq 0.96$. Here, the thixotropy effects are evident, where it is observed that dead zones at the corner of expansion are advected into the channel with increase in thixotropic effects. For unyielded regions in the center of the channel, thixotropic effects also show evident. With the breakdown of the material structure due to stresses generated on the edge of the expansion plan, yielded regions are perceived. With the restructuring of the fluid in the center of the channel, due to the low stresses applied to the fluid in this region, unyielded regions are formed. For less thixotropic cases the formation of unyielded regions are clearly faster (Lagrangian sense) than for more thixotropic cases.

In Fig.**??** shows the results for the structured parameter field for $\theta_0^* = 5 - 100$ and kinematics, elasticity, shear thinning fixed. In a preliminary analysis can perceive structured regions around the center of the channel and the upper corner formed by the area increase in the expansion plan. These regions have low stresses and strain rates, making a insufficient frame for a great breakdown of the structure. For more elastic materials flows are seen fields with higher structured regions both upstream to downstream of the expansion compared to materials with less elasticity.

Fig. **??** shows the influence of the elasticity in the yielded/unyielded zones for the same parameters of the previous results. We can observe that the pattern shown by the structure parameter field is reflected in the morphology of the yielded/unyielded zones. A small growth of the unyielded regions upstream of the expansion plan for materials with

ISSN 2176-5480

Figure 5. Unyielded Regions: τ^*-isobands for $\theta_0^* = 5$, $J = 500$, $n = 0.5$ and: (a)$t_{eq}^* = 0.01$; (b) $t_{eq}^* = 1$ and (c) $t_{eq}^* = 10$

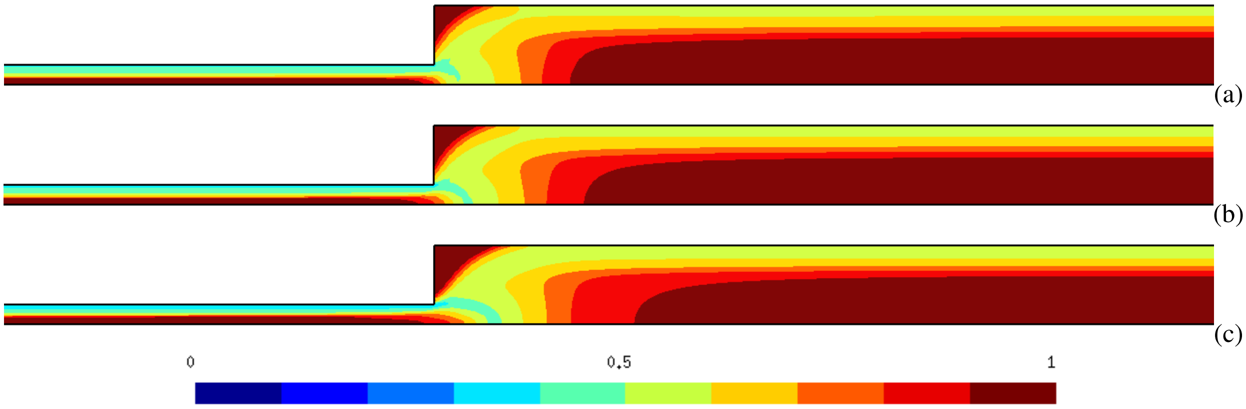

Figure 6. Structure Parameter field for $t_{eq}^* = 1$, $J = 500$, $n = 0.5$ and: (a)$\theta_0^* = 5$; (b) $\theta_0^* = 25$ and (c)$\theta_0^* = 100$

greater elasticity. It is also observed an increase of the unyielded regions in expansion corner to higher levels of elasticity. Downstream of the expansion plan, a formation later of unyielded regions are seen with increased elasticity.

Figure 7. Unyielded Regions: τ^*-isobands for $t_{eq}^* = 1$, $J = 500$, $n = 0.5$ and: (a)$\theta_0^* = 5$; (b) $\theta_0^* = 25$ and (c)$\theta_0^* = 100$

The next results show the influence of the jump number, J, in the Structured Thixotropic creeping flow flow in an abrupt planar expansion. Fluids with lower J have higher levels of structuring. For larger J, a break in the structure more pronounced in the expansion can be observed. By definition, a change in the number jump provides a change of η_0^* level, which influence its level of structure in a state of equilibrium, and therefore the structured parameter field. For this reason it is interesting that we are analyzing the structural viscosity field.

Analyzing Fig.9 we can confirm the above allegations. By analyzing the definition of structural viscosity, Eq. 6, makes it clear where of the J parameter growth is directly proportional to η_0^* .

4. ACKNOWLEDGEMENTS

The author Cleiton Fonseca is sponsored by CNPq - Brazil

ISSN 2176-5480

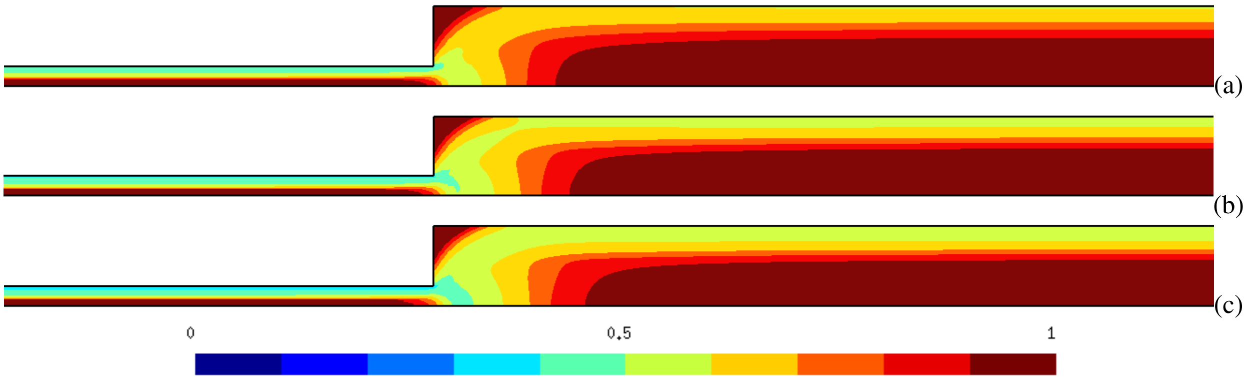

Figure 8. Structure Parameter field for $\theta_0^* = 5$, $t_{eq}^* = 1$, $n = 0.5$ and: (a)$J = 200$: (b)$J = 500$ and (c) $J = 800$

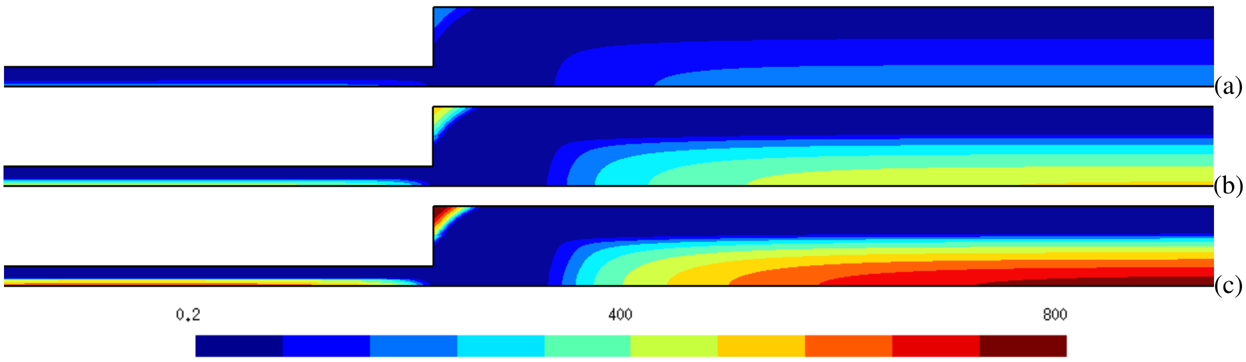

Figure 9. Structured Viscosity isobands for $\theta_0^* = 5$, $t_{eq}^* = 1$, $n = 0.5$ and: (a)$J = 200$: (b)$J = 500$ and (c) $J = 800$

5. REFERENCES

Behr, A.M., Franca, L.P., Tezduyar, T.E., 1993. "Stabilized finite element methods for the velocity–pressure–stress formulation of incompressible flows", Computer Methods in Applied Mechanics and Engineering, vol. 104, pp. 31-48.

De Souza Mendes, P.R., Dutra, E.S.S., 2004. "Viscosity Function for Yield-Stress Liquids", Applied Rheology, vol. 14, pp. 296-302.

De Souza Mendes, P.R., 2007. "Dimensionless non-Newtonian fluid mechanics", Journal of Non-Newtonian Fluid Mechanics, vol. 147, pp. 109-116.

De Souza Mendes, P.R., 2009. "Modeling the thixotropic behavior of structured fluids", Journal of Non-Newtonian Fluid Mechanics, vol. 164, pp. 66-75.

Fonseca, C., Frey, S., De Souza Mendes, P.R., Naccache, M.F., 2013. "Flow of elasto-viscoplastic thixotropic liquids past a confined cylinder", Journal of Non-Newtonian Fluid Mechanics, vol. 193, pp. 80-88.

Franca, L.P., Frey, S., 1992. "Stabilized finite element methods: II. The incompressible Navier-Stokes equations", Comput. Methods Appl. Mech. Engrg., vol. 99, p. 209-233.

Franca, L.P., Valentin, F., 1999. "On an Improved Unusual Stabilized Finite Element Methods for the Advective-Reactive-Diffusive Equations", Comput. Methods Appl. Mech. Engrg., vol. 190, p. 1785-1800.

6. RESPONSIBILITY NOTICE

The authors are the only responsible for the printed material included in this paper.